Iron(II) triggered conformational changes in Escherichia coli fur upon DNA binding: a study using molecular modeling

Article *in* Journal of Molecular Graphics and Modelling · November 2006

DOI: 10.1016/j.jmgm.2005.12.010 · Source: PubMed

2 authors, including:

Mazen Y. Hamed
Birzeit University
33 PUBLICATIONS **280** CITATIONS

SEE PROFILE

Available online at www.sciencedirect.com
ScienceDirect
Journal of Molecular Graphics and Modelling 25 (2006) 234–246
Journal of Molecular Graphics and Modelling
www.elsevier.com/locate/JMGM

Iron(II) triggered conformational changes in *Escherichia coli* fur upon DNA binding: a study using molecular modeling

Mazen Y. Hamed *, Salih Al-jabour

Computational Science Program, Chemistry Department, Birzeit University, PO Box 14, Birzeit, Palestine

Received 21 September 2005; received in revised form 19 December 2005; accepted 20 December 2005
Available online 27 January 2006

Abstract

In order to identify the Fur dimerization domain, a three-dimensional structure of the ferric uptake regulation protein from *Escherichia coli* (Fur EC) was determined using homology modeling and energy minimization. The Fur monomer consists of turn- helix -turn motif on the N-terminal domain, followed by another helix–turn–helix–turn motif, and two β-strands separated by a turn which forms the wing. The C-terminal domain, separated by a long coil from the N-terminal, and consisting of two anti parallel β strands, and a turn–helix–turn–helix–turn motif.

Residues in central domain were found to aid the dimer formation, residues 45–70 as evident in the calculated distances; this region is rich in hydrophobic residues. Most interactions occur between residues Val55, Leu53, Gln52, Glu49 and Tyr56 with closest contacts occurring at residues 49–56. These residues are part of an α-helix (α_4) near the N-terminal.

Upon raising the Fe^{2+} concentration the binding of Fur dimer to DNA was enhanced, this was evident when, the Fur EC dimer was docked onto DNA ''iron box'' (it was found to bind the AT-rich region) and upon addition of Fe^{2+} the helices near the N-terminal bound to the major groove of the DNA. Addition of high Fe^{2+} concentration triggered further conformational changes in the Fur dimer as was measured by distances between the two subunits, Fe^{2+} mediated the Fur binding to DNA by attaching itself to the DNA. At the same time DNA changed conformation as was evident in the distortion in the backbone and the shrinking of major groove distance from 11.4 to 9.3 Å.

Two major Fe^{2+} sites were observed on the C-terminal domain: site 1, the traditional Zn site, the cavity contains the residues Cys92, Cys95, Asp137, Asp141, Arg139, Glu 140, His 145 and His 143 at distances range from 1.3 to 2.2 Å. Site 2 enclave consists of His71, Ile50, Asn72, Gly97, Asp105 and Ala109 at very close proximity to Fe^{2+}.

The closest contacts between Fur dimer and DNA at the AT-rich region were at residues Ala11, Gly12, Leu13, Pro18 and Arg19 mostly hydrophobic residues near the N-terminal domain. Close contacts repeated at His87, His88 and Arg112, and a third region near the C-terminal at Asn137, Arg 139, Glu140, Asn141, His143, Asn141 and His145. Fur dimer has three major contact regions with DNA, the first on the N-terminal domain, a second smaller region at His87, His88 and Arg112 mediated by Fe^{2+} ions, and a third region on the C-terminal domain consisting mainly of hydrophobic contacts and mediated by Fe^{2+} ions at high concentration.

Keywords: Ferric; Uptake; Repressor; Protein; Corepressor; Regulation; DNA

1. Introduction

Fur protein from *Escherichia coli* K12 (Fur EC) is a 17 KDa, 148 amino acid residues protein [1]. Fur EC has attracted much attention in recent years [1–7] and it has been extensively studied as a repressor protein which uses Fe^{2+} as co-repressor to bind specifically to DNA [2–6], it was especially studied with the 19 bp iron box (5′-GAT AAT GAT AATC ATT ATC-3′) [2,8–13]. Other divalent transition metal ions such as Mn^{2+}, Co^{2+} were found to activate Fur both in vitro and in vivo with varying degrees, while Zn^{2+}, Cd^{2+} and Cu^{2+} were found to bind Fur strongly and activated Fur in vitro only [1,5,18]. The X-ray structure of Fur protein from *E. coli* is still not resolved; the NMR studies gave insight about the structure of FurEC and its relation to the Fur function [13–15]. An X-ray structure on a member of the Fur family from *Rhizobium leguminosarum* was reported [16]. The first crystal structure of Fur from *P. aeruginosa* in complex with Zn^{2+} was determined at a resolution of 1.8 Å [17]. X-ray absorption spectroscopic measurements and micro PIXE analysis were also performed

* Corresponding author. Tel.: +972 22 98 2003; fax: +972 22 98 2084.
E-mail address: mhamed@birzeit.edu (M.Y. Hamed).

1093-3263/$ – see front matter © 2006 Elsevier Inc. All rights reserved.
doi:10.1016/j.jmgm.2005.12.010

[17,45] in order to characterize the distinct iron binding sites in solution and it was found to bind four Zn^{2+} ions per Fur dimer with N/O ligands at an average metal–ligand distance of 2.1 Å.

Experimental work revealed many aspects about the Fur structure-function relationship. The HTH motif near the N-terminus was suggested to play the DNA binding role similar to other repressor proteins (λ repressor, DtxR, lac repressor [20–22] and IdeR [24]. Other reports provided insight on the metal ion-binding sites provided by Fur and the role of metal ion in the DNA binding process [25]. Indeed, previous work based on thermodynamic equilibrium gave evidence that Fe^{2+}, Mn^{2+}, and Co^{2+} ions are weakly bound to Fur and ^{57}Fe Mössbauer study showed that Fe^{2+} is present in an axially distorted octahedral environment with $\partial = 1.3\ mms^{-1}$ $\Delta = 1.3\ mms^{-1}$ [5,7,26]. These values, when compared with reported values for Fe^{2+} sites, indicated a moderately bound Fe^{2+} to oxygen and/or nitrogen ligands [23]. This is consistent with the reversible metal ion-binding (K_d value 55 μM [5]) which agrees well with the role of Fur protein as metal ion sensor. Site multiplicity and flexibility was not ruled out as more than one ion was found to bind per Fur [5]. Other metal ions could replace Fe^{2+} as co-repressors and was active in various degrees [1].The proposed role of metal ion was interpreted as to trigger conformational changes in the Fur protein dimer and consequently facilitate DNA binding. Coy [12], basing his study on proteolytic enzymatic cleavage suggested that the metal ion role was to induce conformational changes, and also proposed that both DNA binding and N-terminal sensitivity of Fur were dependent on the metal ion concentration. He also suggested that the C-terminal was responsible for metal ion binding [12]. Most workers [12,17,24,25] tend to agree that Fur has three major domains based on its function; an N-terminal which is responsible for the DNA binding process, a middle domain which plays a role in the dimerization of Fur and the C-terminal which contains the metal ion-binding sites. C-terminal plays the role of metal ion concentration sensing and binding. In this work, the three-dimensional structure of Fur was built using molecular dynamics. The dimerization of Fur was performed in water to produce the Fur dimer. The dimer was studied in the presence of DNA with and without the presence of Fe^{2+} ion. The effect of metal ion on the conformational changes of Fur and how does this act to enhance the DNA binding process at elevated Fe^{2+} concentration and the unbinding of Fur dimer to DNA at reduced Fe^{2+} concentration [44].

In this work, computational methods were used to establish the structure function relationship of Fur protein and to give insight on the mechanism of repressor activity of the Fur dimer upon varying the concentration of the co-repressor (Fe^{2+}). The effect of metal ion on the protein and DNA conformations is established. The most pronounced effect of metal ion at elevated concentrations is the observed distortions took place in DNA which would translate into decreased synthesis of bacterial mRNA.

1.1. Computations and homology modeling

All the molecular dynamics (MD) simulations were performed using AMBER7 molecular simulation package [27,28]. An AMBER force field was used for molecular minimization and molecular dynamics. The analyses of MD trajectories were also preformed by AMBER7. Pymol molecular viewer package was used for visualization [29]. All other calculations were performed on a single-CPU Pentium III machine with Linux platform.

1.2. Homology modeling of Fur protein

The known Fur sequence (from *E. coli*) was submitted to different modeler servers in order to predict the three-dimensional structure. SWISS-MODEL [30], PHD, 3DPSSM [31] and VADAR servers were used to align the Fur sequence with similar known proteins Data Bank. Several templates for Fur protein were generated while the sequence with high similarity served as a reference sequence. The superposition of each atom was optimized by maximizing C_α in the common core while minimizing their relative mean square value deviation (RMSD) at the same time. Spare part algorithm was used to search for fragments that can be accommodated into the framework of the Brookhaven Protein Data Bank (PDB). The coordinates of central backbone atoms (N, O and C) were averaged, and then added to the target model. The side chains were added according to the sequence identity between the model and the template sequence. AMBER7 was used to idealize the geometry for bonds and also to remove any unfavorable non-bonded contacts. This was done by minimizing the energy. All hydrogen atoms were added and the apoFur structure was subjected to a refinement protocol with constraints on the Fur structure gradually removed. 100 steps of steepest descent, followed by 300 steps of conjugate gradient algorithm were applied during energy minimization. The energy minimization process on the apoFur model was performed, first in vacuum and second in H_2O as solvent, nine Na^+ ions were added to the model to neutralize the system.

1.3. Building the Fur dimer

AUTODOCK 2.4 [32] was used to generate the apoFur dimer. Two molecules of the previously determined structure for the apoFur monomer were docked on each other, and the best docking sites were predicted. Monte Carlo (MC) simulated annealing (SA) algorithm was used for exploring the Fur configuration by a rapid energy evaluation technique using a grid-based molecular affinity potential. The energy of interaction, affinity and the grid for electrostatic potential were evaluated using the Poisson–Boltzmann finite difference method and were assigned to each atom.

1.4. Docking of the apoFur dimer onto a 19 bp fragment representing the DNA

Nucgen suite program (part of the AMBER7 package [28]) was used to build the Cartesian coordinates for canonical B- model of the iron box (a 19-bp inverted repeat sequence designated the iron box (5′ GATAATGATAATCATTATC 3′); the proposed recognition site of Fur on the DNA. The

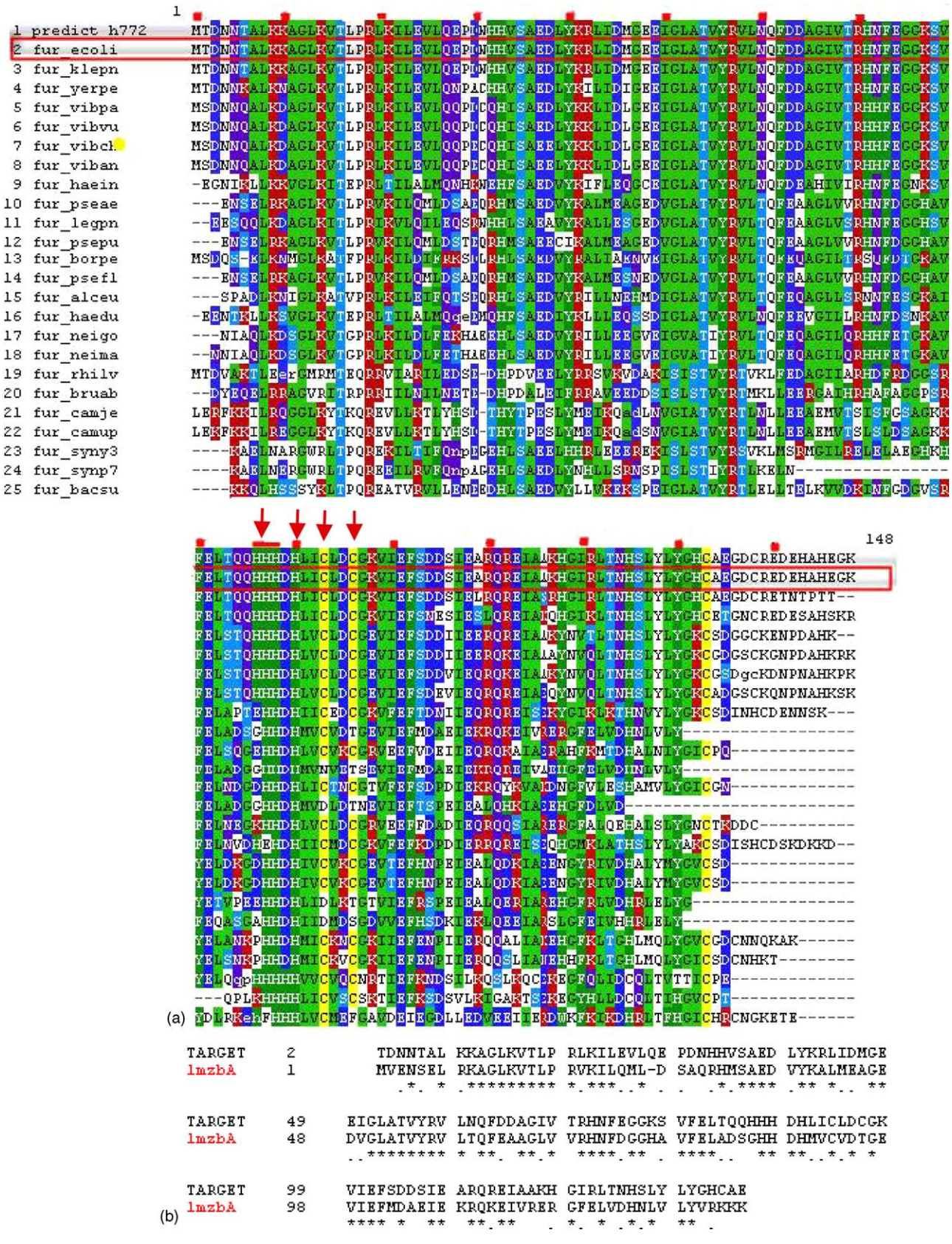

Fig. 1. (a) An alignment of iron acquisition subfamily and that of Fur_*E. coli* protein. Domain predicted using SWISS-MODEL server, hydrophobic residues, green. Cystein yellow, hydrophobic acidic(D and E), dark blue. hydrophilic basic K and R, red. Polar uncharged,purplel and light blue. His, green back ground with white text. (b) Alignment of Fur E.C with Fur P.A [17] PDB code :1 MZB.

right-handed B-DNA duplex conformation was applied for the model. The iron box was docked to the Fur-dimer using the AUTODOCK program. The energy minimization was applied to the resultant model in order to refine the Fur dimer –DNA complex. The parameters file for the iron metal was built manually and inserted into AMBER7 as a library file. The first scenario was using 4 Fe^{2+} ions per Fur dimer–DNA complex in the water environment and adding Na^{+}. MD simulations were carried out at 300 K. Explicit solvent model WATBOX216 water was used as solvent model. The models were solvated with a 10 Å water cap from the center of mass of the ligands. The dynamics simulation was applied for 25 ps time limit. In a second scenario, the same was repeated using 8 Fe^{2+} ions and simulation was applied for 25 ps.

2. Results and discussion

2.1. Calculated Fur EC structure in relation to other known structures in the Fur family

The Fur sequence was submitted to several servers in order to study the preserved amino acid residues in the Fur family. The results of alignment as presented in Fig. 1 showed highly preserved residues in both the N-terminal and C-terminal domains, these residues must play a crucial role in the Fur function as an iron regulator. Comparison of the amino acid sequence of homologous proteins indicates which of the proteins' residues are essential to its function, which are of less significance and which have little specific function, invariant residues uniquely suit essential function of the protein, other residues, conservatively substituted have less stringent side chain requirements [17,22]. On the other hand, other amino acid residues have nonspecific function ''hypervariable''. The main feature is the preserved hydrophobic residues (AGLIV) on 17 positions on the N-terminal domain and to less extent (4 major positions) on the C-terminal domain. Hydrophilic basic residues Lys and Arg (residues Lys9, Lys10), Lys14, Arg19X Lys 21), (Lys41, Lys(Arg42), Arg57, Arg70, Lys77 are repeated 7 times on the N-terminal domain, and once on the C-terminal Arg110XLys112. We can say that proteins in the Fur family are mostly hydrophobic and their N-terminal domains are more hydrophobic than their C-terminal domains. All proteins in the Fur family appear to be Histidine rich [14,15], His32 (replaced by Gln or Glu in some proteins), His33 is preserved and important to Fur function. Indeed, the His33Leu mutant reported to be inactive in vivo [6]. His71, His86, His87, motif His88AspHis90, and His135 are fully conserved, while His142 occurrence is less frequent. The unit Cys93LeuAspCys96Gly is present in a coil folding and is highly preserved in the Fur family. Its worth noting that it was reported by Coy et al [6] that the Cys92Ser Cys95Ser mutations altered the Fur activity drastically, which confirms that Cys92 Cys95 residues are essential to the Fur activity. Glutamic acid 81and Cys132 are also preserved in the Fur family. Some of the homology modeling results for folding coincided with those predicted by NMR spectroscopy [13–15] specifically for coil T_2, α_3, T_3, α_4, and α_5.

The Fur secondary structure was predicted as shown in Fig. 2, especially the conserved region, and compared with those predicted by NMR [13–15]. The results of the homology modeling [35–37] (Fig. 2 and Table 1) using different servers coincided with each other to a great extent and this allowed us to propose a three-dimensional structure for the Fur monomer see Fig. 3. The fitted structure was in good homology with winged helix proteins with an RMSD value of 1.3 Å which falls within the accepted value for protein alignment 1–2 Å. The three-dimensional structure of Fur agrees with its proposed function; the N-terminal domain contains the HTH motif. Most servers gave an α-helix for the residues 4–6 with good confidence level, a coil for residues 11–16 and another α-helix for residues 17–27 another coil 29–35. Another, α-helix for the residues 49–59 followed by coil (60–64), these regions

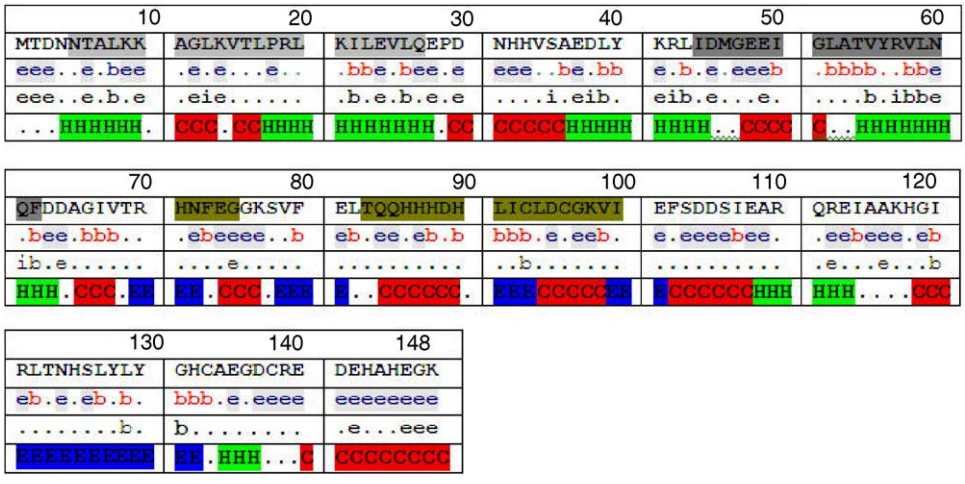

Fig. 2. Fur secondary structure : Row 1 represents the amino acid residues: DNA binding residues Dimerization region iron (II) binding region. Row 2 contains the predicted solvent accessibility composition (core/surface ratio) for Fur protein : (e) residues exposed with more than 16% of their surface, (b) all other residues. Row 4 contains the observed relative solvent accessibility, where b = 0–9%, i = 9–36%, e = 36–100% . predicted solvent accessibility composition and observed relative solvent accessibilty calculated by PROF server [47].Row 5 contains the predicted secondery structure from different servers (high confidance predictions only). Helix, H, coil, C, Beta-strand, E.

Table 1
Results of homology modeling of Fur from different sources compared to that predicted by NMR study [13–15] ; column 2 shows the proposed role reported for each domain in literature

Residues near N-terminal[a]		Folding predicted by NMR [15]	Folding	Confidence level
4–6	DNA binding HTH motif wing		α_1-Helix H1	9
11–16			Coil T_1	8–9
17–27			α_2-Helix H2	9
29–35		Coil	Coil T_2	9
36–44		Helix α	α_3-Helix H3	9
47–51 (G)	Dimerization Region Y55–F61	44–48 coil	Coil T_3	9
52–63	suggested DNA binding domain [15]	49–59 helix 60–64 coil	α_4-Helix H4	9
65,66,67		65–74 helix	Coil T_4	8–9
Residues near C-terminal		**NMR predicted**	**Folding**	**Confidence level**
69–72			β_1-Sheet	6–8
74–76 LYS	Metal ion-binding sites		Coil T_5	8–9
78–81			β_2-Sheet	9
83–89 contain His			Coil T_6	8
90–93 contain His and Cys 92			β_3-Sheet	8
94–98, Cys 95			Coil T_7	8–9
99–101			β_4-Sheet	8–9
102–107			Coil T_8	8–9
108–113		107–117 helix α	α_5-Helix H5	7,8–9
118–120			Coil T_9	7,9,6
121–132			β_5-Sheet	9
134–136			α_6-Helix H6	8,8,7
140–148			Coil T_{10}	7, most 9

[a] Residue numbering is shifted by one in our case , in literature reports ,usually the first residue M is ignored, for example, C92 is labeled C93.

included in the central domain which was reported to be responsible for Fur dimerization [8,12]. In the C-terminal domain two α helices were found in the region 108–113 and 134–136 separated by a β-strand in the region 121–132 and a coil between 118–120. The comparative protein calculations

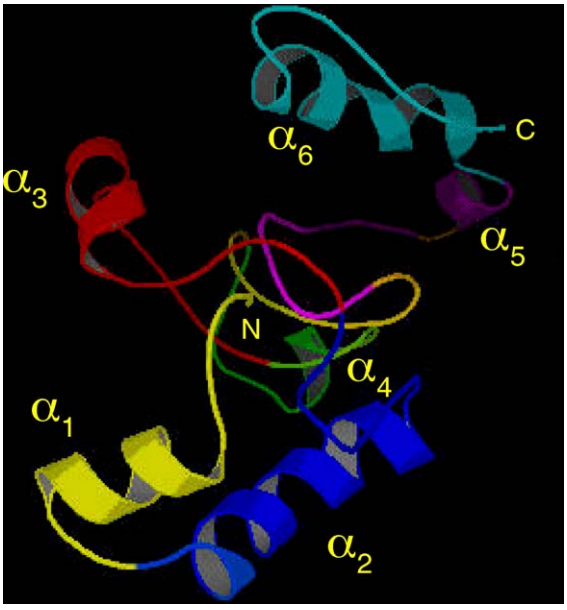

Fig. 3. The three-dimensional structure of the Fur monomer from *E. coli*. A structure generated using homology modeling procedure. SWISS MODEL server Starting from N-terminal coil , α_1 yellow, α_2 blue, α_3 red, α_4 green, α_5 magenta, and α_6 aquamarine. This labeling was in comparison with the DNA binding-domains of DtxR, CAP, λ-repressor and GH5 in reference [22].

gave 67.57% of the Fur residues are exposed to solvent, and this is especially clear for residues forming the loops and residues at both C- and N-terminal domains. 32.43% of Fur protein residues were buried (Fig. 2). The Fur EC sequence was aligned with the Fur sequence from *Pseudomonas aeruginosa* with known crystal structure [17] which was found to bind Zn^{2+} in two different binding sites and does not have sequence similarity with Fur EC, the results of alignment shown in Fig. 1b gave 62.9 % sequence identity. The similarity with high confidence level was for residues Lys10–Pro19, Gly48–Thr54, His71–Ser79, Thr84–Ala110, and Arg121–Gly136. Most important preserved residues are His89, His90AspHis91 and Cys92 (Fig. 1b). Calculated surface area for Fur EC using Spdv software was 7016 $Å^2$ and the volume was 16863 $Å^3$, a cavity of volume 14 $Å^3$ and area 34 $Å^2$ was formed by residues Cys93XY Cys96*, His71–Glu74, and His86–His90.

The amino terminal domain of Fur shares considerable similarity with DtxR [22]; both proteins are iron-dependant repressor proteins but differ in their DNA specific binding [20,22]. Although both of these proteins regulate iron uptake. The Fur monomer (Fig. 3) resembles a great deal the determined structure of DtxR [22] which contains two clearly defined domains, the amino terminal domain consists of 72 residues and contains three helices, two antiparallel β-strands plus the first half of α_4. The second domain (70 residues) contains α_4, α_5 and α_6. The structure contains helix–helix interactions; α_1 with α_4 and α_5, α_2 with α_4, and α_1 with α_5 thought to be crucial for protein function, some interactions between helices of Fur were observed by NMR spectroscopy but were not very pronounced [22,13–15].

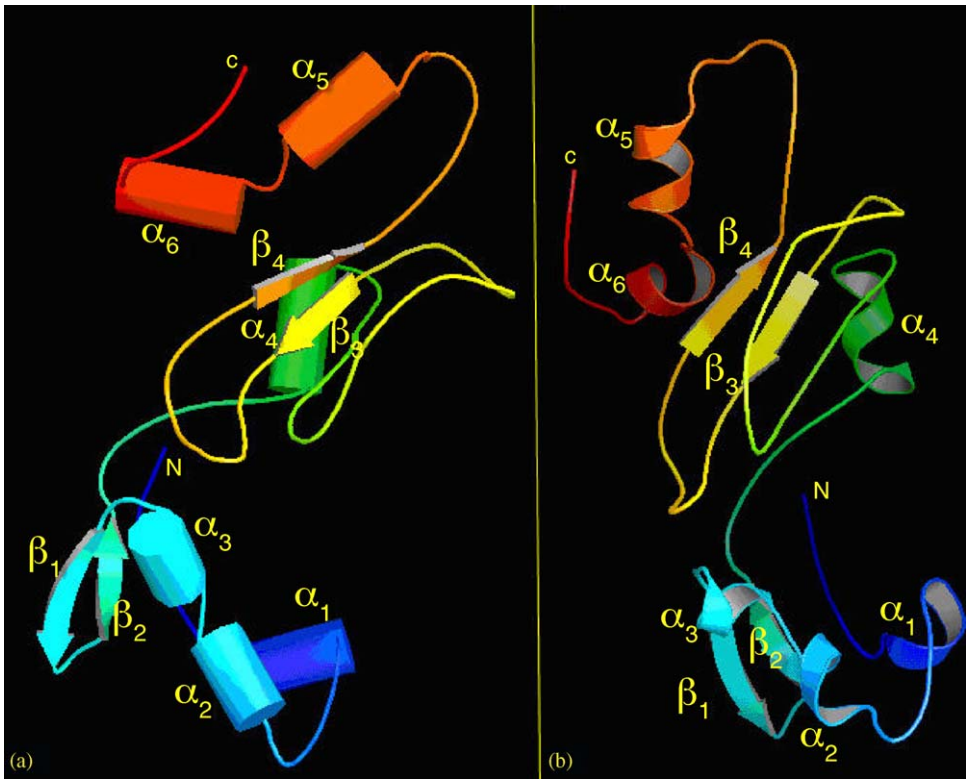

Fig. 4. The three-dimensional structure of Fur protein monomer from *E.coli* at minimum energy calculated using AMBER7 in a water box. (a) Three-dimensional structure of Fur using cartoon representation. (b) Using ribbon display. Publication colors: starting from the N-terminal domain: Blue α_1, cyan α_2, α_3, β_1, β_2, cyan-gradual to green, α_4 green, β_3 yellow β_4 orange α_5 light red, α_6 red.

2.2. Molecular modeling of the Fur protein using molecular dynamics

The three-dimensional structure of the Fur monomer which resulted from homology modeling with the known Fur structures was used as the starting structure in calculations using AMBER7 software, the calculated three-dimensional structure for Fur monomer at minimum energy is shown in Fig. 4. The energy minimization idealized the geometry of bonds and removed unfavorable connections. Energy minimization was applied in a water box. Indeed, an X-ray structure of Fur protein dimer from *Rhizobium leguminosarum* [16] has shown two discrete domains with N-terminal formed from association of two HTH motifs, a flexible hinge linked a compact C-terminal consisting of α/β domain, and a solution X-ray scattering in reducing environment [18] showed that the two domains are flexibly arranged with respect to each other, and no structural homology with DtxR [22] or IdeR [24] apart from that expected HTH motif in the N-terminal. There is also an interface region consisting of polar residues with large void in the core lined by basic residues. In contrast to the N-terminal, the C-terminal formed from a large and stable domain subunit with the role of maintaining the dimerization of Fur. The classic HTH motif consists of two helices (α_1, α_2) joined by loop. It is found that HTH is a conserved domain which binds the DNA [46]. The HTH motifs alone is apparently insufficient for independent folding, a third helix (α_3) stabilizes the motif as a compact, globular domain. The HTH motif followed by two β-hairpin wings reported in the Fur structure which shows a high similarity with winged-helix family.[1]

The folding as resulted from Amber minimization
(1–8) Coil T_1, (9–17) helix* α_1, (18–22) coil T_2*, (23–26) helix* α_2
(27–29) coil T_3, (30–33) helix α_3, (34–36) coil T_4, (37–40) strand+ β_1, (41–42) coil+ T_5 (43–46) strand+ β_2, (47–55) coil T_6, (56–60) helix α_4, (61–90) coil T_7
(91–95) strand β_3, (96–107) coil T_8, (108–111) strand β_4, (112–121) coil T_9 (122–127) helix α_5, (128–131) coil T_{10}, (132–141) helix α_6, (142–148) coil T_{11}

* Helix turn helix motif.

\+ Wing.

2.3. Fur dimer structure

Two Fur monomers were docked on each other using AutoDock [32] and minimizing the energy. The features of the Fur structure are in good agreement with its function as a repressor protein which uses Fe^{2+} or other divalent transition metal ions as co-repressors, i.e., binds the DNA at high Fe^{2+} concentration and falls off the DNA at lower iron concentrations. The structure of Fur dimer (Fig. 5) shows that each subunit is composed of an amino-terminal DNA-binding domain, an interface-domain in the middle and a carboxyl-terminal which

[1] Usually referred to in the literature as C92 and C95.

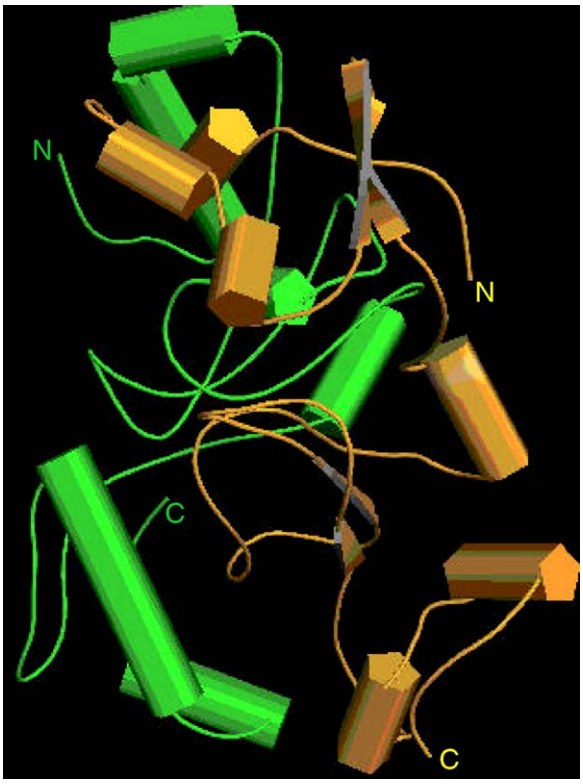

Fig. 5. Fur dimer structure in a water box generated using Autodock. It shows that the closest distances occur at the central domain of each monomer while N- and C-terminal domains in each monomer are pointing away from each other. Colors: one subunit is in gold color, the other is in green.

Table 2
Conformational changes of Fur EC dimer induced by DNA and Fe^{2+} binding as indicated by distances between the residues on one subunit relative to the accompanying residue on the other

Residue	Apo Fur dimer	Apo Fur dimer/DNA	Fur dimer/DNA + $4Fe^{2+}$	Fur dimer/DNA + 8 Fe^{2+}
N-terminal–N-terminal	20.4	15.4	10.6	10.3
$\alpha_1 \rightarrow \alpha_1$[a]	18.3	16.4	10.9	9.2
$\alpha_2 \rightarrow \alpha_2$	10.8	6.5	4.8	2.4
Val25–Val25	3.2	5.60	3.10	3.9
Pro29–Pro29	0.5	1.7	1.5	1.5
$\alpha_3 \rightarrow \alpha_3$	27.5	15.6	17.3	11.0
$\alpha_4 \rightarrow \alpha_4$	13.2	12.7	10.1	8.9
Leu52–eu82	0.7	1.2	1.6	1.2
Gly51–ln85	0.02	0.02	0.5	0.5
Glu49–lu81	0.02	0.4	0.09	0.09
Thr54–Thr83	0.5	1.2	0.9	0.7
Glu49–Glu49	18.2	12.8	10.2	8.2
Thr69–Thr69	12.1	9.5	8.4	8.0
Gln85–Gln85	32.4	34.5	20.4	19.2
Ala53–Ile107	8.60	13.7	12.7	12.5
Thr54-Glu108	9.50	11.8	9.3	8.9
$\alpha_5 \rightarrow \alpha_5$	33.5	34.6	20.8	19.2
Arg112–Arg112	12.7	10.2	8.5	7.6
$\alpha_6 \rightarrow \alpha_6$	34.9	32.1	15.7	14.8
C-terminal–C-terminal	34.9	32.7	15.6	14.2

The calculated distances between residues on each monomer of the Fur dimer. The first column for apoFur dimer, 2nd column for apoFur dimer with DNA; the last two columns show the distances after adding Fe^{2+}.

[a] Helix–helix distance was measured centre to centre.

contains the metal binding sites. Each DNA-binding domain contains the helix–turn–helix motif with a topology similar to other repressor proteins (DtxR, λ repressor,) [22,24]. The resultant apoFur dimer model shows helix–helix interactions at residues 45–60 between the two monomer subunits. This behavior is similar to other proteins; i.e. helix–helix interactions are found in the dimerization domain [17,22,24].

Residues in central domain were found to aid the dimer formation, specifically residues 45–70 as evident in the calculated distances (Table 2, Figs. 5 and 11), this region is rich in hydrophobic residues. Most interactions occur between residues Val55, Leu53, Gln52, Glu49 and Tyr56 with closest contacts occurring at residues 49–56. These residues are part of an α-helix (α_4) near the N-terminal. Indeed Coy and Neilands

Table 3
Distances between Fur residues and AT of DNA: column (A) apoFur dimer/DNA (no iron present)

Residue distance (Å)	(A) Fur dimer/DNA	(B) Fur dimer/DNA + $4Fe^{2+}$ distance (Å)	(C) Fur dimer/DNA + 8 Fe^{2+} distance (Å)
N-terminal	7.8	5.8	4.3
Ala11	0.9	1.0	0.8
Gly12	0.8	0.7	0.5
Leu13	0.7	0.7	0.4
Pro18	1.3	1.3	1.6
Arg19	7.4	6.9	6.4
His32	8.6	7.8	7.7
His33[a]	8.5	7.5	6.8
Arg57[b]	7.5	5.4	4.3
Gln61[c]	11.2	9.9	9.6
Phe62[b]	10.2	8.3	7.3
Ile67[c]	11.2	8.2	7.4
Arg70	19.3	17.5	16.6
Phe73	9.6	8.4	7.4
His86	3.4	2.6	1.9
His87	4.1	2.8	2.3
His88	3.7	2.1	1.8
D89[d]	3.9	3.2	2.5
H90[d]	4.1	3.4	2.9
Arg112	34.5	30.3	28.9
Ile114	27.3	25.9	25.2
Ile120	23.0	20.3	19.4
His125	32.8	30.6	21.3
Gly131	29.5	27.2	27.5
His132[a]	8.9	4.5	3.2
Asp137	4.2	2.3	1.9
Arg139	4.9	2.3	2.1
Glu140	4.2	3.2	2.2
Asp141	5.1	2.5	1.6
His143[e]	4.5	2.7	1.8
His145	5.3	3.1	1.7
C-terminal	24.5	20.4	17.5

Column (B) Fur dimer/DNA + $4Fe^{2+}$. Column (C) Fur dimer/DNA + 8 Fe^{2+}.

[a] Residues reported by NMR shift of aromatic region [13] to bind negatively charged phosphate backbone.

[b] Reported to reside in the recognition helix interacting directly with DNA [38].

[c] bind phosphate backbone as reported by change in aliphatic carbon NMR shift [13].

[d] Possible ligands for iron(II) in regulatory site in vivo as reported by Bsat and Helmann [43].

[e] Reported by NMR shift not to bind DNA [13].

[12] and Kolade et al. [16] suggested that the helix–helix interactions occur at the central domain closer to the N-terminal. The negatively charged and highly polar glutamic acid residue seems to aid the establishment of hydrogen bonding a cross Fur subunits. Extensive hydrophobic interactions occur between the two monomers aided by the hydrophobic properties of valine and leucine. The aromatic ring of tyrosine also helps to establish hydrogen bonding between the two monomers [17,38]. To the contrary of what was predicted by NMR spectroscopy [13], the N-terminal from each subunit is at close proximity to the other and at large distance from the C-terminal.

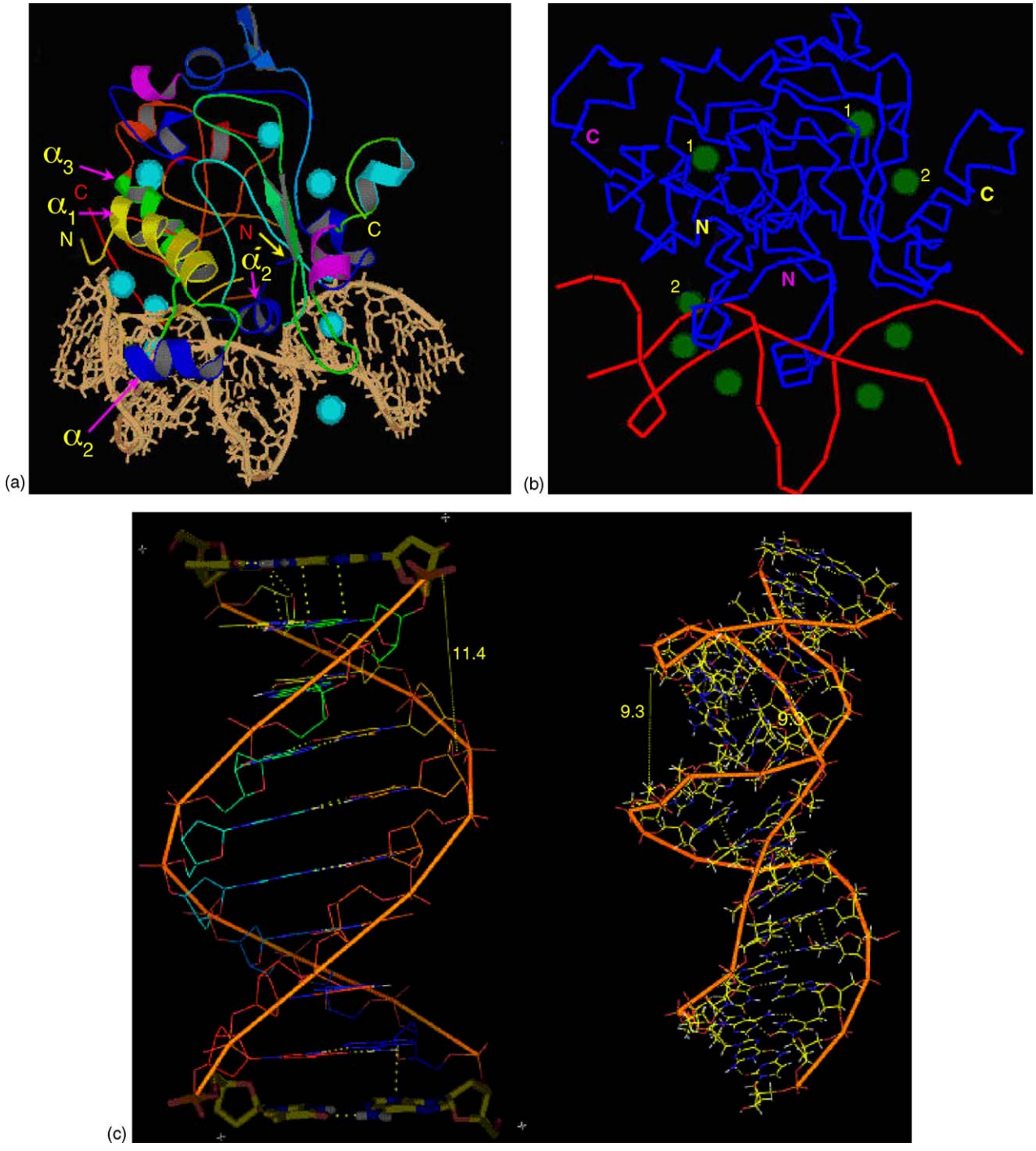

Fig. 6. (a) The interaction of the Fur dimer with DNA in the presence of Na^+, $8Fe^{2+}$ ions and using H_2O as solvent. The α_2-and α_2'-helices (blue) interact with the AT-rich region of the major groove of the conical B-DNA (iron box). (b) line structure of the Fur dimer interacting with DNA, conditions as in (a) This figure shows the major Fe^{2+} sites 1 and 2, and the other four Fe^{2+} ions are close to the DNA. (c) Tilting of DNA in the presence of Fur dimer, 8 Fe^{2+}, Na^+ in water: The three-dimensional structure of the conecial B-DNA, before binding to the Fur dimer (left) and after binding the Fur dimer (right). The calculated distances between phosphates in the backbone in the first major groove of the two models are shown.

2.4. DNA Binding

The Fur EC dimer was docked onto a DNA iron box (5′ GATAATGATAATCATTATC 3′) in the presence of water and Na^+ ions and measuring the contacts between Fur residues and DNA, the results are shown in Tables 2 and 3. It is clear from the measurements that when Fe^{2+} ions were added to the Fur/DNA complex, it resulted in an obvious tuning of the Fur structure This constituted a conformational change, obviously triggered by the addition of Fe^{2+} ions (see Table 2). The outcome was to bring the HTH motif near the N-terminal in close proximity to the major grooves of the DNA. As a result of this process, the Fur dimer engulfed the DNA, see Table 3 and Fig. 6. Upon the addition of another four Fe^{2+} ions, the change in conformation was more evident and the helices moved closer to the major groove of DNA. This proved without doubt that the process, i.e., the Fur dimer specific binding to DNA depends on the concentration of Fe^{2+} [11–13,19,25]. A critical issue in terms of the structure–function relationship of Fur is how the regulator interacts with its operator site to block the access to the promoter region of an iron-responsive gene [25]

The Fur dimer/DNA model clearly suggested that the putative DNA-binding helices α_2 and α_2' contact the major groove of DNA [11,12,25]. The model shows that α_2 and α_2' fit well into the major groove (Fur changes conformation to

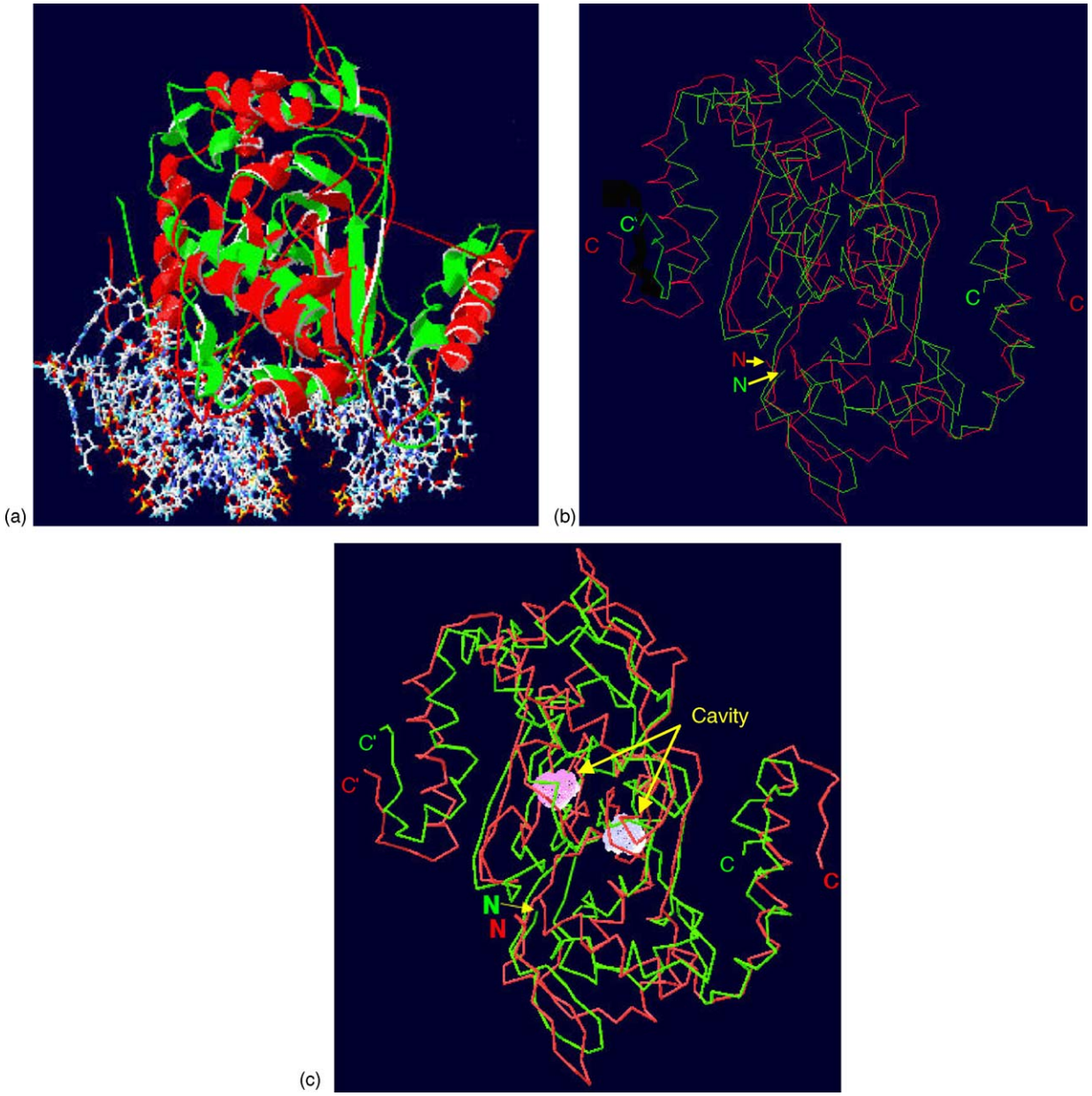

Fig. 7. (a) Conformational changes in Fur dimer upon binding to Fe^{2+} and DNA: The Fur dimer DNA complex no Fe^{2+} present (red) and after adding 8Fe^{2+}ions (green). (b) Two models of the three-dimensional structure of the Fur dimer displayed in line mode. Before adding Fe^{2+} (red) the conformational changes appear between the two models. After adding 8 Fe^{2+} ions and DNA binding (green) (c) The same model as in Fig. 6b showing the cavities Lilac colored cavity is for red model before adding Fe^{2+}, and the off-gray cavity for the green model after adding the 8 Fe^{2+}, the shift in cavity position upon adding iron is apparent.

prevent their overlap). Recognition and binding is the result of direct interactions between the base pairs in the major groove of DNA and the amino acid side chains of α_2 and α_2' helices (Fig. 6). The calculated distances showed specific contacts taking place between the side chains of Val15, Leu13, Ala11 and Pro 18 and DNA, see Table 3. The cyclic pyrrolidine side group of proline 18 undergoes hydrogen bonding to the AT base pairs spaced by 4 base pairs [2,24,25,39,40,41,44]. While the hydrophobic properties of valine, leucine and alanine residues made the hydrophobic interactions between Fur and edges of the bases and sugar-phosphate backbone of DNA groove possible [25]. These interactions induce an affect on the DNA by over winding the four base pairs in the middle (Fig. 6c). As a result, the minor groove in the center of the operator was compressed in a way that the phosphate to phosphate distance was reduced from 11.4 Å for canonical B-DNA to 9.3 Å upon Fur dimer binding (Fig. 6c) [25].

Types of Fur contacts with DNA Operator sequence were analyzed experimentally by several workers [9–12,42] using ethylation and hydroxyl radical foot printing and was found to be similar to the unique HTH motif and these contacts were found to be on one face of DNA [42] and span three major grooves [11,12], indeed this is clearly observed in our calculated structure shown in Figs. 6 and 7, the Fur dimer clamps around the major grooves of DNA using an α_2-helix from each monomer. When the nature of the residues which contacts with DNA were analyzed the following can be said about the Fur DNA complex: A striking structural feature (a pair of two-fold α-helices were tilted and has center to center separation of 2.4 Å. α_2-helices were also located at very close proximity to DNA so that the N-terminal chain and side chains were able to make nonspecific contacts with phosphate diester backbone see Fig. 6, Tables 2 and 3, the common DNA binding structure is still the HTH motif in which the contacts can result from hydrogen bonds, salt bridges and van der Waal forces. All these forces account for site recognition and specific binding. Additional nonspecific contacts attributed to the loose loops on both ends of Fur dimer: residues near the C-terminal (see Table 3) loops work as an arm to engulf the DNA.

The change in DNA conformation is worth noting as the tilting which took place upon Fur binding in the presence of Fe^{2+}, H_2O and Na^+ is evident and the major groove distance shrunk from 11.4 to 9.3 Å, a notable conformational change is evident as can be seen in Fig. 6c this was interpreted in some reports as a hand shake between Fur and DNA [25].

2.5. Iron (II) binding sites on the Fur dimer

The addition of Fe^{2+} ions to the Fur dimer/ DNA complex induced a change in conformation of the Fur structure as evident in the distances between residues and helices of the Fur subunits in the dimer (Table 2) (Figs. 7a,b and 11b). The N-terminal domains were at 20.6 Å apart in the apoFur dimer, they moved closer to each other by 5 Å upon addition of DNA. Upon adding the first 4 Fe^{2+} ions a significant move took place; the N-terminals became at 10.6 Å apart. At the same time residues moved closer to the DNA. The addition of the first 4 Fe^{2+} ions per Fur dimer could produce a significant change in Fur conformation. The Fur dimer/DNA complex in the presence of water and Na^+ ions, could take up to 8 Fe^{2+} ions per complex, the more Fe^{2+} ions added, the closer the Fur subunits became to the DNA. This was accompanied by conformational changes in both Fur dimer and DNA.

The nature of ligands provided by the Fur dimer to metal ion, and the number of metal ion sites were always a matter of debate [5] and it is worth the attention as it plays a key role in the whole process. There are two major sites provided by the Fur dimer to Fe^{2+}, site 1 which involves Cys92 and Cys95 and other residues with N or O ligands (Table 4, Fig. 9). Cys92 and Cys95 were always reported to play a crucial role in metal ion binding and Fur function [5,6,12,13,18,19,23,43]. Indeed, a Fur mutant with either or both Cys92 and Cys95 replaced by Ser lost its repressor activity and failed to bind the DNA [6]. Both Cys92 and Cys95 are present in a β-strand and a loop, respectively near the C-terminal domain and they are relatively

Table 4
Calculated distances between Fe^{2+} and closest residues on the Fur for the first two iron ions added

Residue	Position of residue in structure	Donor atom (type of interaction)	Residue-Fe(II) Distance (Å)
Site 1 (Zn site)			
Fe–Cys92	Coil	H-bonded H_2O	2.2
Fe–Cys95	Coil	H-bonded H_2O	1.6
Fe–Asp137	Coil	O	1.3
Fe–Asp141	Coil	O	1.5
Fe–Arg139	Coil	N	1.7
Fe–Glu140	Coil	O	1.3
Fe–His145	Coil	N	1.2
Site 2			
Fe–His71	End of β-strand	N	1.3
Fe–Ile50	Coil	Hydrophobic	2.3
Fe–Asn72	β-Strand	N	1.5
Fe–Gly97	Coil	Polar	2.3
Fe–Asp105	Coil	O	1.4
Fe–Ala109	α Helix	Hydrophobic	2.1
Other residues at close proximity to iron			
Fe–His32	α helix	N	3.6
Fe–His33[a]	α-helix	N	4.2
Fe–Arg57	α-helix	N	5.1
Fe–Gln61	Coil	N, O	4.9
Fe–Phe62	Coil	Hydrophobic	7.9
Fe–Ile67	Coil	Hydrophobic	8.3
Fe–Arg70	Coil	N	3.4
Fe–Phe73	Coil	Hydrophobic	3.1
Fe–Ile114[b]	Coil	Hydrophobic	4.9
Fe–Ile120[b]	Coil	Hydrophobic	6.2
Fe–His132[a]	α-helix	N	5.4
Fe–His86	Coil	N	4.1
Fe–His87	Coil	N	3.7
Fe–His88	Coil	N	4.2
Fe–H90[c]	Coil	N	3.9
Fe–D89[c]	Coil	O	4.2

[a] The largest effect on NMR shift was observed for H33 upon addition of Mn^{2+} [13].
[b] Considerable change in NMR shift was observed upon titrating Fur-Mn^{2+} with DNA [13].
[c] Possible ligands for iron(II) in regulatory site in vivo as reported by Bsat and Helmann [43].

buried inside the protein as can be seen in Fig. 2. EXAFS results [18] suggested a metal environment consisting of a total of 5 oxygen and nitrogen atoms at an average distance of 2.13 Å (either 2O at 2.05 Å/3N at 2.17 Å or 3O at 2.08 Å/2N at 2.19 Å). In our study, the calculated distances were Fe^{2+}–Cys92 = 2.2 Å and Fe^{2+}–Cys95 = 1.6 Å (Fig. 8c). Cysteines are probably bound through H-bonded H_2O intermediate or a protonated SH as indicated by the weak binding evident in the Mössbauer parameters for Fe^{2+} and the reported dissociation constant which ruled out the presence of strong sulfur–Fe^{2+} bonds [5]. His143 and His145 were close to the DNA and it seems that they form part of the iron-binding environment [43] (Fig. 8d). The calculated distances show that these residues moved closer to the DNA upon metal binding. Aspartic (Asp137–Asp141), Arg139 and glutamic acid (Glu140) complete the distorted octahedral environment around Fe^{2+}. Another Fe^{2+} is coordinated by the side-chains of residues His71 (end of β-strand), Asp105 (coil), Ala109 (α-helix), Asn72 (β-strand) and Ile50 (coil) [43] (Fig. 8b). This site is probably site 2 with O and N bound to Fe^{2+} in a distorted octahedral environment. Table 3 shows the calculated distances between the donor atoms of these residues and Fe^{2+} ions; His71 plays an important binding role to Fe^{2+}. Recent experimental reports suggested that apoFur contains at least one Zn^{2+} ion per monomer coordinated to Cys92 and Cys95 and another metal ion-binding site which contains iron [17–19,23,34,43]. Site 1 is the Zn^{2+}-binding site while (Fur was reported to contain structural Zn^{2+} ion per monomer [33,34]) the other site is an Fe^{2+} site. Another reported Zn^{2+} binding site which involves Cys132 and Cys137 in the C-terminal domain [17,45] could not be found in our study. The excess Fe^{2+} bind the phosphate backbone in AT- rich region of the minor groove, see Figs. 8c,d and 9. It is evident that the Fe^{2+}, in this case, acts as mediator for the binding of Fur residues to the DNA, and at the same time participate in conformational changes of DNA.

The metal ion and HTH binding to major grooves play an important role in inducing conformational changes of the canonical B-DNA [25]. Recent studies proved the presence of strongly bound Zn^{2+} ion to the Fur [18,33] the suggested site is 1 and its tetrahedrally bound to both C92 and C95 and other residues. This made what used to be apoFur dimer to be active in vitro without adding Fe^{2+} [43].

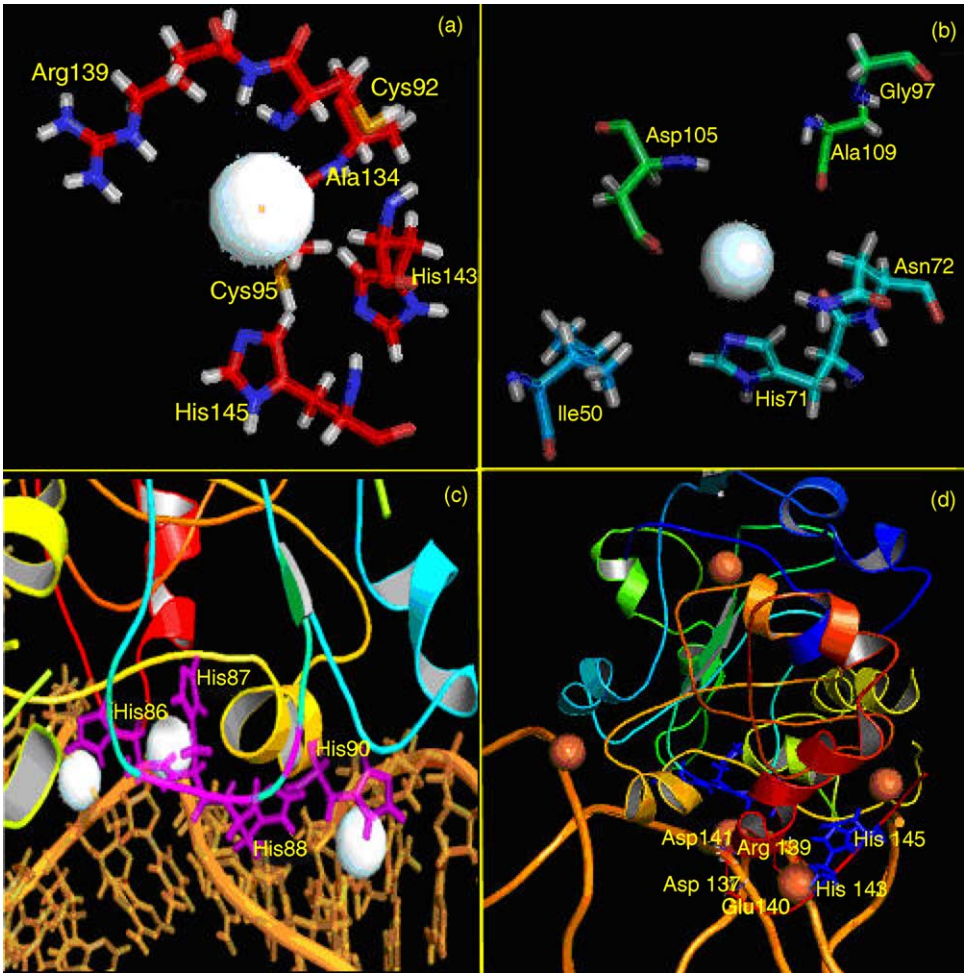

Fig. 8. (a) Close-up view of the coordination at metal binding site 1. (b) Close-up view of metal site 2. (b) Close-up view of the residues and Fe^{2+} near the DNA. A metal ion is present between His86, His87, His89 and His90 and AT of DNA (for distances see Tables 3 and 4). The recognition site for Fe^{2+} the motif His86His87His88Asp89His90 binds DNA mediated by Fe^{2+} [43] (c) Close-up view of Fe^{2+} site 1 close to the DNA. Ligands provided by C-terminal are Asp137, Arg139, Glu140, Asp141, and His145, Fe^{2+} ion in DNA groove shown in bright green (calculated distances are shown in Tables 3 and 4).

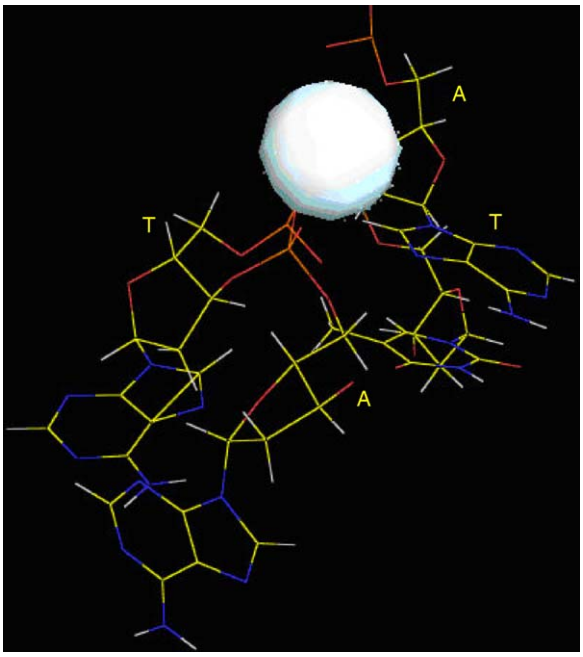

Fig. 9. Close-up view of Fe^{2+} binding to DNA (AT region) at elevated concentration, conditions as in Fig. 6.

2.6. Evidence for conformational changes triggered by DNA binding and metal ion binding

In the presence of DNA the Fur dimer changes conformation before adding the Fe^{2+} as can be seen in Fig. 11. Residues on the sub units move closer together except for Val25–Val25, Pro29–Pro29, Gln85–Gln85, Ala53–Ile107 and α_5–α_5 moved apart. Upon adding low Fe^{2+} concentrations all residues and helices

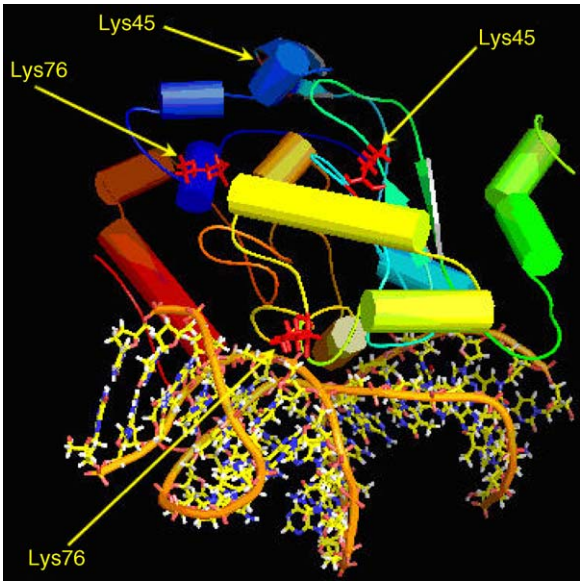

Fig. 10. The Fur dimer binding to DNA in the presence of Na^+, H_2O and $8Fe^{2+}$. Testing the effect on Lysine45 and Lys76 hydrophobic residue which was reported by de Peredo et al. [38]. Lys76 proved to be highly protected from modification upon Fur DNA binding (Lys76 present in the wing and may interact with DNA). The result was interpreted as change in Fur conformation upon activation.

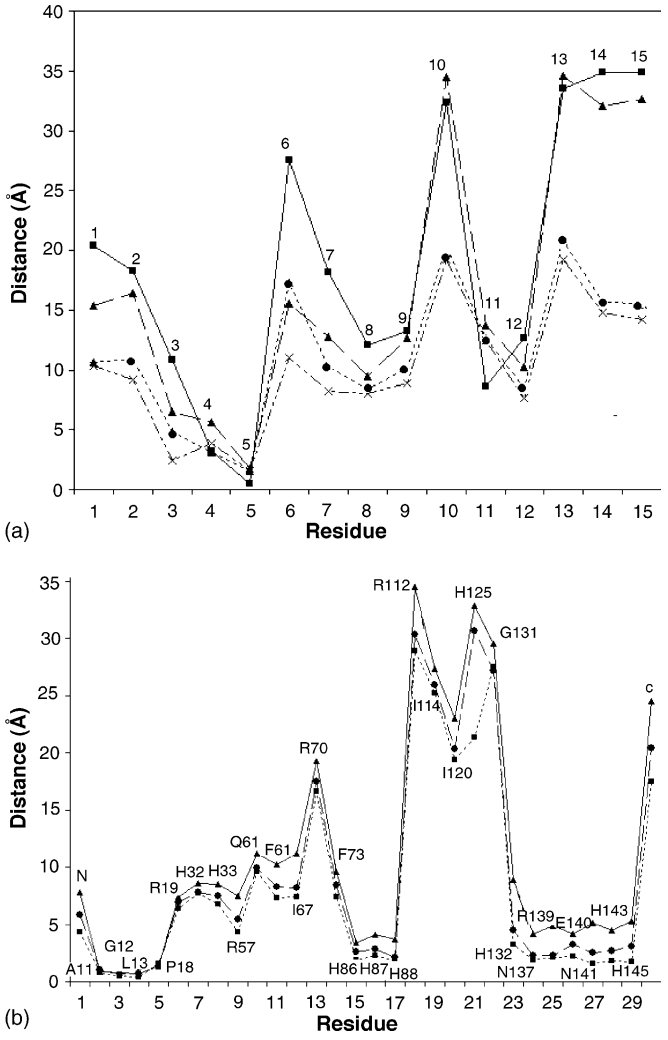

Fig. 11. (a) Conformational changes of the Fur EC induced by DNA and Fe^{2+} binding. Distance between residues and helices on one Fur subunit and the other. ApoFur dimer (■). ApoFur/DNA (▲). Fur/DNA in the presence of 4 Fe^{2+} ions (●) and Fur/DNA in presence of 8 Fe^{2+} ions (×). Labels on the plots are as follows: N-terminal–N-terminal (1), α_1–α_1 (2), α_2– α_2 (3), Val25–Val25 (4), Pro29–Pro29 (5), α_3– α_3 (6), Glu49–Glu49 (7), Thr69–Thr69 (8), α_4–α_4 (9), Gln85–Gln85(10), Ala53–Ile107 (11); Arg112–Arg112 (12),; α_5–α_5(13), α_6–α_6 (14), C-terminal–C-terminal (15). (b) Conformational changes of the Fur EC dimer and DNA binding. Calculated distances between the amino acid residues of Fur and the AT-unit in the B-canonical DNA (Table 3). Fur dimer and DNA fragment (▲) (continuous line). Fur dimer and DNA in the presence of 4 Fe^{2+} ions (●) (broken line). Fur dimer and DNA in presence of 8 Fe^{2+} ions (■) (dotted line). This plot show that residues Ala11, Gly12, Leu13 Pro18 and Arg19 near the N-terminal, His88 to Arg112, and the residues139–145 near the C-terminal are the closest to DNA.

on the Fur subunits move closer together causing a drastic change in conformation. The addition of larger concentration of Fe^{2+} shifted the subunits closer but the move was less drastic than when the first Fe^{2+} were added (Fig. 10).

The N- and C-terminals behave in different manner, the N–N moved drastically towards each other upon adding the DNA and the first Fe^{2+} addition but the second Fe^{2+} addition did not cause much change in the N–N distance. The C–C distance shifted slightly upon DNA binding, while the drastic shift in distance was when the low Fe^{2+} concentration was added and a similar shift occurred when more Fe^{2+} was added. The inter phase

region showed considerable rigidity as can be seen in Fig. 11 (Val 25, Pro 29 and α_4–α_4), no considerable change in distances was observed.

The closest contacts between Fur dimer and DNA at the AT-rich region were at residues Ala11, Gly12, Leu13, Pro18 and Arg19 mostly hydrophobic residues near the N-terminal domain. Another close contacts repeated at His87, His88 and Arg112 and a third region engulfs the DNA near the C-terminal at Asn137, Arg139, Glu140, Asn141, His143, Asn141 and His145. As can be observed in Fig. 11b Fur dimer has three major contact regions with DNA, the first on the N-terminal domain, a second smaller region at His87, His88 and Arg112 mediated by Fe^{2+} ions as shown in Fig. 8c and a third region on the C-terminal domain consisting mainly of hydrophobic contacts and mediated by Fe^{2+} ions at high concentration.

Acknowledgements

We wish to thank the Amber group in UCSF for providing the software, and Pymol Prof. Arthur J. Olson, DeLano Scientific California for the Pymol viewer.

References

[1] A. Bagg, J.B. Neilands, Biochemistry 26 (1987) 5471–5477.
[2] L. Escolar, J. Perez-Martin, V. de Lorenzo, J. Mol. Biol. 283 (3) (1998) 537–547.
[3] Y.M. Hamed, J. Inorg. Biochem. 51 (594) (1993) 1–2.
[4] M.Y. Hamed, J.B. Neilands, J. Inorg. Biochem. 53 (4) (1994) 235–248.
[5] M.Y. Hamed, J.B. Neilands, V. Huynh, J. Inorg. Biochem. 50 (3) (1993) 193–210.
[6] M. Coy, C. Doyle, J. Besser, B.J. Neilands, BioMetals 7 (1993) 292–298.
[7] L. Jacquament, F. Dole, C. Jeandey, J.L. Oddou, E. Perret, L. La Pape, D. Aberdam, J.L. Hazemann, I. Michaud-Soret, J.M. Latour, J. Am. Chem. Soc. 122 (2000) 394–395.
[8] J.B. Neilands, Can. J. Microbiol. 38 (7) (1992) 728–733.
[9] E. Le Cam, D. Frechon, M. Barray, A. Fourcade, E. Delain, Proc. Natl Acad. Sci. U.S.A. 91 (25) (1994) 11816–11820.
[10] D. Frechon, E. Le Cam, Biochem. Biophys. Res. Commun. 201 (1) (1994) 346–355.
[11] M. Coy, Biochem. Biophys. Res. Commun. 212 (3) (1995) 784–792.
[12] M. Coy, J.B. Neilands, Biochemistry 30 (33) (1991) 8201–8210.
[13] T. Saito, R.J.P. Williams, Eur. J. Biochem. 197 (1991) 43–47.
[14] T. Saito, M.R. Womlad, R.J.P. Williams, Eur. J. Biochem. 197 (1991) 29–39.
[15] T. Saito, R.J.P. Williams, D. Duly, Eur. J. Biochem. 197 (1991) 39–42.
[16] O.O. Kolade, P. Bellini, M. Wexler, A.W.B. Johnston, J.G. Grossmann, A.M. Hemmings, Biometals 30 (4) (2002) 771–774.
[17] E. Pohl, J.C. Haller, A. Mijovilovich, W. Meyer-Klaucke, E. German, M.L. Vesil, Mol. Microbiol. 47 (4) (2003) 903–915.
[18] L. Jacquamet, D. Aberdam, A. Adrait, J.L. Hazemann, J.M. Latour, I. Michaud-Soret, Biochemistry 37 (1998) 2564–2571.
[19] E.E. Zheleznova, J.H. Crosa, R.G. Brennan, J. Bacteriol. 182 (21) (2000) 6264–6267.
[20] M.P. Schmitt, E.M. Twiddy, R.K. Holmes, Proc. Natl. Acad. Sci. USA. 89 (10) (1992) 7576–7580.
[21] J.F. Reidhaar-Olsin, R.T. Sauer, Proteins: Struct. Funct. Genet. 7 (1990) 306–316.
[22] X. Qiu, C.L.M.J. Verlinde, S. Zhang, M.P. Schmitt, R.K. Holmes, W.G.J. Hol, Structure 3 (1) (1995) 87–100.
[23] L. Jacquamet, F. Dole, C. Jeandey, J.L. Oddou, E. Perret, L. Le Pape, D. Aberdam, J.L. Hazemann, I. Michaud-Soret, J.M. Latour, J. Am. Chem. Soc. 122 (2000) 394–395.
[24] G. Wisedchaisri, R.K. Holmes, W.G.J. Hol, J. Mol. Biol. 342 (4) (2004) 1155–1169.
[25] R.G. Brennan, B.W. Matthews, TIBS 80 (1988) 6513–6517.
[26] D. Barondeau, E.D. Getzoff, Curr. Opin. Struct. Biol. 14 (6) (2004) 765–774.
[27] D.A. Case, D.A. Pearlman, J.W. Caldwell, T.E. Cheatham III, J. Wang, W.S. Ross, C.L. Simmerling, T.A. Darden, K.M. Merz, R.V. Stanton, A.L. Cheng, J.J. Vencent, M. Crowley, V. Tsui, H. Gohlke, R.J. Radmer, Y. Duan, J. Pitera, I. Massova, G.L. Seibel, U.C. Singh, P.K. Weiner, P.A. Kollman, Amber, 7, University of California, San Francisco, 2002.
[28] D.A. Pearlman, D.A. Case, J.W. Caldwell, W.R. Ross, T.E. Cheatham, I.I.I.S. DeBolt, D. Ferguson, G. Seibel, P. Kollman, Comp. Phys. Commun. 91 (1995) 1–41.
[29] W.L. DeLano, The PyMol Molecular Graphics System on the World Wide Web (2002).
[30] S. Torsten, K. Jürgen, G. Nicolas, C.P. Manuel, SWISS-MODEL: an automated protein homology-modeling server, Nucleic Acids Res. 31 (13) (2003) 3381–3385.
[31] L.A. Kelley, R.M. MacCallum, M.J.E. Sternberg, Enhanced genome annotation using structural profiles in the program 3D-PSSM, J. Mol. Biol. 299 (2) (2000) 501–522.
[32] M.M. Garrett, S.G. David, H. Ruth, E.H. William, H. Scott, B. Rik, J.O. Arthur, Automated docking of flexible ligands to receptors (Autodock). Molecular Graphics Laboratory, Department of Molecular Biology, 10550 North Torrey Pines Road, La Jolla, CA (2002) 92037-1000, Version 3.0.5.
[33] E.E. Zheleznova, J.H. Crosa, R.G. Brennan, J. Bacteriol. 182 (21) (2000) 6264–6267.
[34] E.W. Althaus, C.E. Outten, K.E. Olson, H. Cao, T.V. O'Halloran, Biochemistry 38 (1999) 6559–6569.
[35] G.J. Lesser, G.D. Rose, Proteins: Struct. Funct. Genet. 8 (1990) 6–13.
[36] C.a. Schiffer, J.W. Calwell, P.A. Kollman, R.M. Stroud, Proteins: Struct. Funct. Genet. 8 (1990) 30–43.
[37] M. Akke, S. Forsen, Proteins: Struct. Funct. Genet. 8 (1990) 23–29.
[38] A.G. De Peredo, C. Saint-Pierre, J.M. Latour, I. Michaud-Soret, E. Forest, J. Mol. Biol. 310 (2001) 83–91.
[39] M. Fuangthong, J.D. Helmann, Am. Soc. Microbiol. 185 (21) (2003) 6348–6357.
[40] J.L. Huffman, R.G. Brennan, Curr. Opin. Struct. Biol. 12 (1) (2002) 98–106.
[41] J.L. Lavrrar, C.A. Christoffersen, M.A. McIontosh, J. Mol. Biol. 322 (2002) 983–995.
[42] V. de-Lorenzo, F. Giovannini, M. Herrero, J.B. Neilands, J. Mol. Biol. 203 (1987) 875–884.
[43] N. Bsat, J.D. Helmann, J. Bacteriol. 181 (14) (1999) 4299–4307.
[44] L. Escolar, J. Perez-Martin, V. de Lorenzo, J. Bacteriol. 181 (20) (1999) 6223–6229.
[45] A. Adrait, L. Jacquamet, L. Le Pape, A.G. de Peredo, D. Aberdam, J.L. Hazemann, J.M. Latour, I. Michaud-Soret, Biochemistry 38 (1999) 6248–6260.
[46] N. Baichoo, J.D. Helmann, J. Bacteriol. 184 (21) (2002) 5826–5832.
[47] M. Ouali, R.D. King, Cascaded multiple classifiers for secondary structure prediction, Prot. Sci. 9 (2000) 1162–1176.